The 2009 IEEE/RSJ International Conference on
Intelligent Robots and Systems
October 11-15, 2009 St. Louis, USA

Understanding Robot Motor Capability using Information-Theory-Based Approach

Hsien-I Lin and C. S. George Lee
School of Electrical and Computer Engineering
Purdue University
West Lafayette, IN 47907-2035
{sofin, csglee}@purdue.edu

***Abstract*— Robot skills are usually learned from the so-called learning-from-human-demonstration methods. However, with the limitation of robot motor capability, a robot may not be able to duplicate human motor skills with the same motor performance. To alleviate the problem, one of the possible solutions is to know robot motor capability in advance. Thus, we develop a quantitative measure of a robot motor system, called a pseudo index of motor performance (pI_p), and utilize it to compare with the index of performance (I_p) of a human motor system. To investigate the I_p, we propose an information-theory-based method to characterize a robot motor system. Computer simulations and experiments with a PUMA 560 robot will be conducted to validate the proposed information-theory-based method.**

***Index Terms*— Robot motor capability, pseudo index of performance, information-theory-based.**

I. INTRODUCTION

In robotics, skills the an ability to perform sensory-motor coordination and control to accomplish a desired task [1], [2]. Skills are usually learned by the so-called learning-from-human-demonstration methods [3]–[5]. These methods include learning from demonstration, learning by imitation, and social learning. In these methods, they assume that robots have the sufficient motor capability, and by observing human movements, basic characteristics in skills can be “captured and transferred” to robots to generate the same skill movements.

However, a robot has the limitation of motor capability due to the configuration of its kinematics, dynamics, and control. Thus, the robot may not be able to acquire skills from human demonstration with the same motor performance. In addition, human-demonstrated tasks are usually consisted of rapid aimed movements. Thus, it becomes important to quantitatively examine the intrinsic properties of rapid aimed movements of human motor skills and understand how they relate to the intrinsic properties of robot motor skills, rather than to learn human skills by merely observing human movements. To provide a quantitative measure of rapid aimed movements for a robot motor system, the paper proposes an information-theory-based method inspired by Fitts' law [6] to discover the intrinsic quantitative properties of robot motor skills and their representation of robot motor capability.

For human rapid aimed movements, Paul Fitts [6] in 1954 revealed his experimental results showing the information capacity of a human motor system, which is the ability to produce consistently a class of movements from several alternative classes of movements. In his experiments, he obtained the information capacity of a human motor system by measuring the variability of successive responses that the human aims to produce, and the variability of motor performance is described by two main factors, speed and accuracy. Fitts obtained the following equation, often called Fitts' law, as

$$T_{mt} = a + b \cdot \log_2(\frac{2D}{W}) \quad (1)$$

where T_{mt} is the minimum movement time, a and b are proportional constants, and Fitts quantitatively defined an index of task difficulty (I_d) as $\log_2(\frac{2D}{W})$ (bits/response) to specify the minimum required information for rapid aimed movements to accomplish a given task, where D is a target distance and W is a target width. Then, Fitts defined

$$\frac{1}{T_{mt}} \cdot \log_2(\frac{2D}{W}) \quad (2)$$

as an index of performance (I_p) to indicate the fixed information capacity and found that I_p is relatively constant over a considerable range of movement amplitudes and tolerance limits.

On the robot side, we focus on investigating robot motor performance of rapid aimed movements where a robot performs movements with the maximum movement speed (minimum movement time) to achieve a task constrained by the task spatial accuracy. In this paper, we propose a quantitative measure of a robot motor system, called a pseudo index of motor performance (pI_p) to compare with the index of performance (I_p) of a human motor system for evaluating the feasibility of skill transfer.

This paper is organized as follows. In Section II, we propose an information-theory-based modeling to characterize robot motor capability. In Section III, we present the pseudo index of motor performance (pI_p) and how pI_p is utilized to evaluate the feasibility of transferring rapid

This work was supported in part by the National Science Foundation under Grant IIS-0427260. Any opinion, findings, and conclusions or recommendations expressed in this material are those of the authors and do not necessarily reflect the views of the National Science Foundation.

aimed movements from human demonstration. In Section IV, computer simulations and experiments on a PUMA 560 robot are presented. Conclusions are summarized in Sections V.

II. Information-Theory-Based Method of Robot Motor Capability

Figure 1 shows the information-theory-based method to study the robot motor capacity. In this proposed method, we consider a robot as an information channel that is modeled by its kinematics, dynamics, and control. The desired trajectory is considered as the information at the transmitter and is going to be conveyed through the robot to the receiver. The receiver is the end-effort of the robot. The actual trajectory is the information obtained at the receiver. Since the information channel is disturbed by noises due to the inaccuracy of robot kinematics and dynamics, this results in the trajectory tracking error. The motor capability, which determines how much the actual trajectory will be identical to the desired one, is modeled as the channel capacity of an information channel. The channel capacity determines the maximal error-free data that can be reliably conveyed through the channel. When the capacity is larger, the more error-free data will be obtained at the receiver. For a robot, the larger motor capability makes the actual trajectory more identical to the desired one.

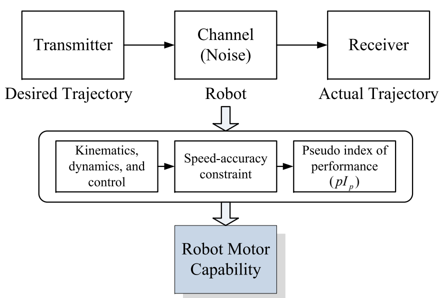

Fig. 1. Proposed information-theory-based approach for the investigation of robot motor capability.

The basic concept of the approach is to estimate the information capacity of a robot system, which determines the robot motor capability. The information capability of the channel is affected by the amount of noises (due to the inaccuracy of kinematics and dynamics models) and assumed as the rate of information transmission from the ratio of the amount of possible responses to the amount of noises. Hence, we utilize a previously-proposed speed-accuracy constraint to characterize the motor capability of a robot. We derive the pseudo index of performance (pI_p) from the speed-accuracy constraint. Since human-demonstrated tasks are usually consisted of rapid aimed movements, and these movements are quantitatively characterized by the index of performance (I_p) of Fitts' law, we can utilize both pI_p and I_p to evaluate whether the robot has the motor capability to cope with skill learning from human demonstration; that is, to move like a demonstrating human with speed and position accuracy as required.

III. Robot Motor Capability Measured by Pseudo Index of Performance

The spatial inaccuracy of the end-effector of a robot with revolute joints is caused by the inaccuracy of robot kinematics and dynamics models. In our previous work, we have investigated the Cartesian position error of the end-effector of an N-DOF manipulator (e.g., a PUMA robot) with revolute joints with robot kinematics, dynamics, and control taken into consideration. When the input for a joint is a ramp function, the Cartesian position error of the end-effector is expressed as [7]

$$\begin{bmatrix} d_x \\ d_y \\ d_z \end{bmatrix} = \boldsymbol{C}(\boldsymbol{\theta}) + \boldsymbol{J_d}(\boldsymbol{\theta})\boldsymbol{K}\triangle\boldsymbol{P}(\boldsymbol{\theta}) + \boldsymbol{J_d}(\boldsymbol{\theta})\boldsymbol{K}\dot{\boldsymbol{\Phi}}^T\triangle\boldsymbol{H}(\boldsymbol{\theta})\dot{\boldsymbol{\Theta}} \tag{3}$$

where $\dot{\boldsymbol{\theta}} = [\dot{\theta}_1, \dot{\theta}_2, \cdots, \dot{\theta}_i, \cdots, \dot{\theta}_N]^T$ and the superscript T denotes a matrix transpose, $\boldsymbol{C}(\boldsymbol{\theta})$ is the kinematic errors due to the mechanical tolerance in manufacturing the links and joints of the robot, $\boldsymbol{J_d}(\boldsymbol{\theta})$ is the Jacobian matrix, $\boldsymbol{K}$ is a matrix whose elements are constants, $\triangle\boldsymbol{P}(\boldsymbol{\theta}) = \triangle\boldsymbol{G}(\boldsymbol{\theta}) + \triangle\boldsymbol{V}$ where $\triangle\boldsymbol{G}(\boldsymbol{\theta})$ is the error between the actual gravity term and its computed term, $\triangle\boldsymbol{V}$ is the error between the actual Coulomb friction and its computed friction at the actuator shaft, $\triangle\boldsymbol{H}(\boldsymbol{\theta}) = \mathrm{diag}\{\triangle\boldsymbol{H}_1(\boldsymbol{\theta}), \cdots \triangle\boldsymbol{H}_{\mathrm{N}}(\boldsymbol{\theta})\}$ where $\triangle\boldsymbol{H}_i(\boldsymbol{\theta})$ is a symmetric matrix whose elements are $\triangle H_{ijk}(\boldsymbol{\theta})$, where j and k are integers, $1 \leq j \leq N$ and $1 \leq k \leq N$, and $\triangle H_{ijk}(\boldsymbol{\theta})$ is the error between the effective velocity-related term and its computed term, $\dot{\boldsymbol{\Phi}} = [\dot{\boldsymbol{\theta}}'_1, \boldsymbol{0}, \cdots, \boldsymbol{0}; \boldsymbol{0}, \dot{\boldsymbol{\theta}}'_2, \boldsymbol{0}, \cdots, \boldsymbol{0}; \cdots; \boldsymbol{0}, \cdots, \boldsymbol{0}, \dot{\boldsymbol{\theta}}'_N]$ where $\dot{\boldsymbol{\theta}}'_i = \dot{\boldsymbol{\theta}}$ for $i = 1$ to N, and $\dot{\boldsymbol{\Theta}} = [\dot{\boldsymbol{\theta}}''_1, \cdots, \dot{\boldsymbol{\theta}}''_N]^T$, where $\dot{\boldsymbol{\theta}}''_i = \dot{\boldsymbol{\theta}}^T$ for $i = 1$ to N.

After the speed-accuracy constraint is obtained, we can derive and calculate the index of performance ($\boldsymbol{I_p^r} = \begin{bmatrix} I_{px}^r, I_{py}^r, I_{pz}^r \end{bmatrix}^T$) of a robot motor system from this constraint, following the same approach that Fitts derived his index of performance I_p (as shown in Eq.(2))

The purpose of determining index of performance $\boldsymbol{I_p^r}$ of a robot motor system is to obtain a quantitative measure compatible with I_p of Fitts' law in bits/time. For a robot motor system, the index of task difficulty (I_d) is defined in the Cartesian space and expressed as

$$\boldsymbol{I_d^r} = \begin{bmatrix} I_{dx}^r, I_{dy}^r, I_{dz}^r \end{bmatrix}^T = \begin{bmatrix} \log_2(\frac{2D_x}{\epsilon_x}) \\ \log_2(\frac{2D_y}{\epsilon_y}) \\ \log_2(\frac{2D_z}{\epsilon_z}) \end{bmatrix}, \tag{4}$$

where $\boldsymbol{D} = [D_x, D_y, D_z]^T$ represents the distance between the start and end positions of a robot movement in the Cartesian space, and $\boldsymbol{\epsilon} = [\epsilon_x, \epsilon_y, \epsilon_y]^T$ are the Cartesian position tolerances. We assume that $\boldsymbol{\theta}_d = [\theta_d^1, \theta_d^2, ..., \theta_d^N]^T$ is the distance between the start and end positions of robot movements in the joint space, and they are obtained from applying the inverse kinematics to these positions. By using a joint-interpolated motion planning, all joints are synchronized by the movement time T_{mt}^r ($T_{mt}^r = \theta_d^1/\dot{\theta}_d^1 = \theta_d^2/\dot{\theta}_d^2 = \cdots = \theta_d^N/\dot{\theta}_d^N$). Referring to the definition of I_p

of Fitts' law (I_d/T_{mt}), the index of performance ($\boldsymbol{I_p^r}$) of a robot motor system is defined as

$$\boldsymbol{I_p^r} = \left[\ I^r_{px}, I^r_{py}, I^r_{pz}\ \right]^T = \left[\begin{array}{c} \log_2(\frac{2D_x}{\epsilon_x})(T^r_{mt})^{-1} \\ \log_2(\frac{2D_y}{\epsilon_y})(T^r_{mt})^{-1} \\ \log_2(\frac{2D_z}{\epsilon_z})(T^r_{mt})^{-1} \end{array} \right]. \quad (5)$$

From Eq. (5), $\boldsymbol{I_p^r}$ includes three indices of performance, I^r_{px} on the x-axis, I^r_{py} on the y-axis, and I^r_{pz} on the z-axis, and we can use one of them as a one-dimensional I_p of a human motor system from Fitts' law. Since $\boldsymbol{I_p^r}$ is represented by bits/time, it becomes possible to quantitatively measure the motor capability of a robot system.

Fitts from his experiments concluded that I_p is relatively constant over a considerable range of movement amplitudes and tolerance limits, but I^r_{px}, I^r_{py}, and I^r_{pz} in Eq. (5) are not constant because of the nonlinear relationship between $\boldsymbol{D}$ in the Cartesian space and $\boldsymbol{\theta}_d$ in the joint space. Thus, to quantitatively indicate the amount of the information capacity of a robot motor system, we derive a pseudo index of performance (pI_p) from the speed-accuracy constraint.

One convention to represent the index of performance (I_p) of Fitts' law in Eq. (1) is defined as $\frac{1}{b}$ by ignoring the constant a. Actually, Fitts' equation is a special case of the quasi-power function with varying exponents n as $n \to \infty$ [8]. The quasi-power function with exponent n is shown as $T_{mt} = a_n + b_n \cdot (\frac{D}{W})^{\frac{1}{n}}$. When $n \to 1$, the quasi-power function becomes a linear function as

$$T_{mt} = a_1 + b_1 \cdot (\frac{D}{W}), \quad (6)$$

which is used to compare with the linear speed-accuracy relationship as

$$W = a^{'} + b^{'} \cdot (\frac{D}{T_{mt}}), \quad (7)$$

where D is the movement distance, T_{mt} is the movement time, W is the effective-width, and $a^{'}$ and $b^{'}$ are proportional constants. For Eqs. (6) and (7), they have a linear relationship. Smaller b_1 results in smaller T_{mt} in Eq. (6), and smaller b' in Eq. (7) if D and W are fixed in both equations. Thus, we define the pseudo index of performance (pI_p) of the linear speed-accuracy equation in Eq. (7) as $pI_p \triangleq \frac{1}{b'}$ to quantitatively indicate the amount of information capacity of a robot motor system. According to the speed-accuracy constraint of a ramp input (see Eq. (3)), $\boldsymbol{C}(\boldsymbol{\theta}) + \boldsymbol{J_d}(\boldsymbol{\theta})\boldsymbol{K}\triangle\boldsymbol{P}(\boldsymbol{\theta})$ can be referred to as a' in Eq. (7), and when we consider that the Cartesian position errors are expressed as positive values and $\dot{\boldsymbol{\theta}}_d = \rho\dot{\boldsymbol{\theta}}_0$ by using a joint-interpolated motion planning (where $\dot{\boldsymbol{\theta}}_0$ is a reference joint velocity vector and $\rho > 0$ is a scalar to change the joint velocities), we can express Eq. (3) in the form of Eq. (7) as

$$\left[\begin{array}{c} d_x \\ d_y \\ d_z \end{array} \right] = \left[\boldsymbol{C}(\boldsymbol{\theta}) + \boldsymbol{J_d}(\boldsymbol{\theta})\boldsymbol{K}\triangle\boldsymbol{P}(\boldsymbol{\theta})\right] + \left[\begin{array}{c} \frac{1}{pI_{px}} \\ \frac{1}{pI_{py}} \\ \frac{1}{pI_{pz}} \end{array} \right] \cdot \rho^2 \quad (8)$$

where pI_{px}, pI_{py}, and pI_{pz} are the pseudo indices of performance on the x-, y-, and z-axis of the Cartesian space, respectively, and are derived as

$$\begin{aligned} pI_{px} &= \left(\boldsymbol{I_x}^T\boldsymbol{J_d}(\boldsymbol{\theta})\boldsymbol{K}\dot{\boldsymbol{\Phi}}_0^T\triangle\boldsymbol{H}(\boldsymbol{\theta})\dot{\boldsymbol{\Theta}}_0\right)^{-1}, \\ pI_{py} &= \left(\boldsymbol{I_y}^T\boldsymbol{J_d}(\boldsymbol{\theta})\boldsymbol{K}\dot{\boldsymbol{\Phi}}_0^T\triangle\boldsymbol{H}(\boldsymbol{\theta})\dot{\boldsymbol{\Theta}}_0\right)^{-1}, \\ pI_{pz} &= \left(\boldsymbol{I_z}^T\boldsymbol{J_d}(\boldsymbol{\theta})\boldsymbol{K}\dot{\boldsymbol{\Phi}}_0^T\triangle\boldsymbol{H}(\boldsymbol{\theta})\dot{\boldsymbol{\Theta}}_0\right)^{-1}, \end{aligned} \quad (9)$$

where $\boldsymbol{I_x}$, $\boldsymbol{I_y}$, and $\boldsymbol{I_z}$ are unit vectors along the x-, y-, and z-axis, respectively, $\dot{\boldsymbol{\Phi}}_0$ is an $N^2 \times N$ matrix and $\dot{\boldsymbol{\Phi}}_0 = [\dot{\boldsymbol{\theta}}_1^{'}, \boldsymbol{0}, \cdots, \boldsymbol{0}; \boldsymbol{0}, \dot{\boldsymbol{\theta}}_2^{'}, \boldsymbol{0}, \cdots, \boldsymbol{0}; \cdots; \boldsymbol{0}, \cdots, \boldsymbol{0}, \dot{\boldsymbol{\theta}}_N^{'}]$ where $\dot{\boldsymbol{\theta}}_i^{'} = \dot{\boldsymbol{\theta}}_0$ for $i = 1$ to N, and $\dot{\boldsymbol{\Theta}}_0$ is an $N^2 \times 1$ matrix and $\dot{\boldsymbol{\Theta}}_0 = [\dot{\boldsymbol{\theta}}_1^{''}, \cdots, \dot{\boldsymbol{\theta}}_N^{''}]^T$ where $\dot{\boldsymbol{\theta}}_i^{''} = \dot{\boldsymbol{\theta}}_0^T$ for $i = 1$ to N.

From Eq. (8), we obtain the quadratic function of the Cartesian position errors, (d_x, d_y, d_z), with respect to the scalar of the joint velocity, ρ. Figure 2 illustrates the obtained quadratic function of the Cartesian position error of the end-effector of a robot along the x-axis (d_x) with respect to the scalar of the joint speed (ρ) where the intercept on the axis of the Cartesian position error of the end-effector of a robot is $\boldsymbol{I_x}^T[\boldsymbol{C}(\boldsymbol{\theta}) + \boldsymbol{J_d}(\boldsymbol{\theta})\boldsymbol{K}\triangle\boldsymbol{P}(\boldsymbol{\theta})]$. From Fig. 2 and Eq. (8), they show that a robot is capable of performing more accurately with a larger pI_p when the joint velocities, $\dot{\boldsymbol{\theta}}_d$, are fixed (i.e., ρ is fixed). In other words, when the Cartesian position tolerances, $\boldsymbol{\epsilon}$, of a given task are fixed (i.e., d_x is fixed), a robot with a larger pI_p is capable of accomplishing the task with faster joint velocities. Interestingly, the pseudo index of performance is advantageous to show the trade-off relationship between speed and accuracy if we assume that there exists a fixed amount of information capacity of a robot motor system.

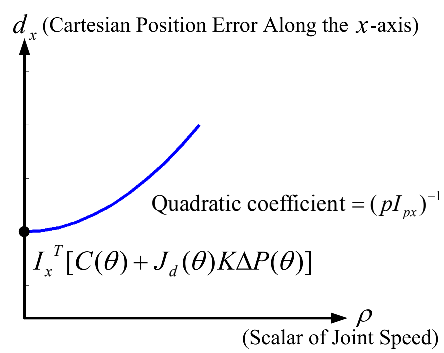

Fig. 2. Quadratic function of the Cartesian position error of the end-effector of a robot along the x-axis (d_x) with respect to the scalar of the joint velocity (ρ) where the quadratic coefficient is $(pI_{px})^{-1}$ and $\dot{\boldsymbol{\theta}}_d = \rho\dot{\boldsymbol{\theta}}_0$.

Figure 3 shows quadratic trajectories for robots with different $pI_{px}{}'s$. In Fig. 3, $pI_{px}{}'s$ of various robots with the same DOFs and $\dot{\boldsymbol{\theta}}_0$ are sorted in order from robot i to robot n after $\boldsymbol{C}(\boldsymbol{\theta}) + \boldsymbol{J_d}(\boldsymbol{\theta})\boldsymbol{K}\triangle\boldsymbol{P}(\boldsymbol{\theta})$ of a robot is subtracted from the Cartesian position errors of the end-effector of the robot along the x-axis where $\boldsymbol{\theta}$ is the target joint position. On the contrary, if $\boldsymbol{C}(\boldsymbol{\theta}) + \boldsymbol{J_d}(\boldsymbol{\theta})\boldsymbol{K}\triangle\boldsymbol{P}(\boldsymbol{\theta})$ of these robots is not subtracted, the comparison of applicability among these robots should be made with $\boldsymbol{C}(\boldsymbol{\theta}) + \boldsymbol{J_d}(\boldsymbol{\theta})\boldsymbol{K}\triangle\boldsymbol{P}(\boldsymbol{\theta})$ taken into consideration.

Figure 3 also shows how to evaluate which robots are able to perform human rapid aimed movements by satisfying the same task spatial-accuracy constraint with the same human movement speed. We assume the direction of the robot movements is along the x-axis. From Eq. (5), I_{px}^{r} of the index of performance of robot i ($\boldsymbol{I_p^r}$) can be calculated and compared with I_p of Fitts' law of human skills in bits/time. If I_{px}^{r} of robot i is less than I_p of a human subject, robots $i+1$ to n are definitively not capable of performing the human rapid aimed movements because they do not have enough motor capability characterized by speed and accuracy constraints.

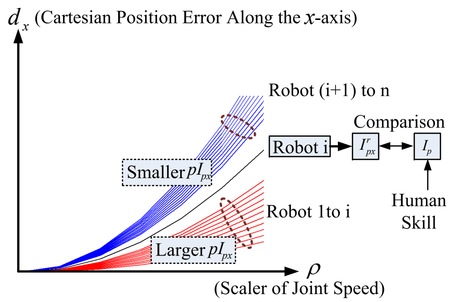

Fig. 3. Quadratic trajectories among robots with different $pI_{px}{}'s$.

IV. Computer Simulations & Experimental Work

Computer simulations and experiments were performed on a PUMA 560 robot to validate and demonstrate that the motor capability can be measured by the proposed pseudo index of performance (pI_p) on a reaching task.

In this experiment, the PUMA 560 robot was asked to perform a reaching task by moving its end-effector to reach a specific point in the three-dimensional space. The task was different from the tapping task performed in Fitts' paper [6]. The difference was that the movement speed and the distance were manipulated in this experiment instead of the movement tolerance and the distance in Fitts' experiment. By controlling movement speed and distance, the Cartesian position errors of the end-effector of the robot were measured to show how they were affected by the movement speed and the distance. From Eqs. (6) and (7), we clearly see that Fitts' experiment was based on Eq. (6) and its manipulated variables were the movement tolerance and the distance and its response variable was the movement time (number of hits on the plate). On the contrary, our reaching task was based on Eq. (7) and the manipulated variables were the movement speed and the distance and the response variable was the movement position error.

Even though the manipulated variables in our experiment and Fitts' experiment are different, the purpose of both experiments aims at utilizing the maximum movement speed to accomplish a task with a specified accuracy criterion. Once the relationships between speed and accuracy are obtained from a human and a robot, respectively, they can be utilized to derive compatible indices of motor performance in terms of bits/sec.

Figure 4 shows the scheme of our task. The robot was asked to move its end-effector to hit a target position (G) and stop at an end position (E) by various configuration of movement speed (D/T_{mt}) and distance (D). With each configuration of movement speed and distance, it resulted in a Cartesian position error (W) at the end-effector. Practically, the robot joint movements had a trapezoidal velocity trajectory. We chose the target position on the constant velocity of the trapezoidal trajectory (G was on joint ramp movements) because the Cartesian position error could be verified by the speed-accuracy constraint in Eq. (3) when joint movements were a ramp function.

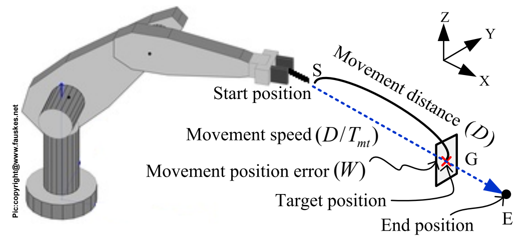

Fig. 4. An experiment for a reaching task. The PUMA 560 robot was asked to hit the target position/region with the specified movement speed, and the Cartesian position error of the end-effector was measured (S: start position, G: target position, and E: end position).

We used a joint-interpolated motion planning for the robot. The start, target, end joint positions were obtained by applying the inverse kinematics to these positions. To be compatible with Fitts' experiments, we utilized inch as the unit of length. The distance between the start (S) and the target (G) positions was set as 2, 4, 8, and 16 inches as the same as in experiment 1 in Fitts' paper [6]. The movement speed (D/T_{mt}, inch/sec) for a specified distance (D) was set as same as Fitts' experiment. For example, when $D=2$, D/T_{mt} was set as $2/0.392$, $2/0.281$, $2/0.212$, and $2/0.180$; when $D=4$, D/T_{mt} was set as $4/0.484$, $4/0.372$, $4/0.260$, and $4/0.203$; when $D=8$, D/T_{mt} was set as $8/0.580$, $8/0.469$, $8/0.357$, and $8/0.279$; when $D=16$, D/T_{mt} was set as $16/0.731$, $16/0.595$, $16/0.481$, and $16/0.388$.

1) Computer simulations on a PUMA 560 robot: We evaluated the pseudo index of performance of a PUMA 560 robot with various $\triangle \boldsymbol{m}'s$ where $\triangle \boldsymbol{m} = \boldsymbol{m} - \boldsymbol{m^c}$, $\boldsymbol{m}$ were the actual masses, and $\boldsymbol{m^c}$ were the computed masses. In other words, a robot with a different $\triangle \boldsymbol{m}$ had different motor capability because Eq. (9) shows that the pseudo index of performance is affected by $\triangle \boldsymbol{H}(\boldsymbol{\theta})$ (i.e., $\triangle \boldsymbol{m}$). To investigate the Cartesian position errors of the end-effector of the PUMA 560 robot caused by the changes of the joint velocities, we subtracted the velocity-independent terms, $\boldsymbol{C}(\boldsymbol{\theta}) + \boldsymbol{J_d}(\boldsymbol{\theta})\boldsymbol{K}\triangle\boldsymbol{P}(\boldsymbol{\theta})$, from the Cartesian position errors at the target position. The parameters of the PUMA 560 robot were taken from [9]. To perform the reaching task, we fixed the target joint positions and changed the start joint positions for $D = 2, 4, 8,$ and 16. The joint velocities were represented as $(\boldsymbol{\theta}_{diff}^{D=2,4,8,16})/T_{mt}$ where $\boldsymbol{\theta}_{diff}^{D=2,4,8,16}$ is the difference between the start and target joint positions for $D = 2, 4, 8,$ and 16 and T_{mt} is the execution time for all joints. If we set $\rho = 1/T_{mt}$, the joint velocities were expressed as $\rho \cdot \boldsymbol{\theta}_{diff}^{D=2,4,8,16}$. We changed ρ by increasing T_{mt} with 0.01 seconds. In the simulations, the joint position, velocity, acceleration, and the inverse dynamics of the robot were calculated by the recursive Newton-Euler equations [10], [11] and the Cartesian position error of the end-effector of the robot was calculated by $\boldsymbol{J_d}(\boldsymbol{\theta})\triangle\boldsymbol{\theta}$.

Figures 5, 6, and 7 show the Cartesian position errors along the x-axis (d_x) with respect to $\rho \cdot D$ when $\triangle \boldsymbol{m}$ was -1%, -0.6%, and -0.2%, respectively. In each figure, sub-figures (a), (b), (c), and (d) represent $D = 2, 4, 8,$ and 16 inches, respectively. In each sub-figure, we used a quadratic function to do curve fitting for our simulation results. We noticed that sub-figures (a), (b), (c), and (d) in each figure had different quadratic coefficients because the unit on the x-axis was $\rho \cdot D$ that was non-linear to joint velocities. The results were similar to the explanation that I_{px}^r is not relatively constant in Eq. (5) because of the nonlinear relationship between D in the Cartesian space and $\boldsymbol{\theta}_d$ in the joint space. Similarly, sub-figures (a), (b), (c), and (d) in Figs. 6 and 7, respectively, had different quadratic coefficients. To avoid the nonlinearity between D and joint velocities, we chose ρ as the unit on the x-axis. Any joint velocity changes were done by changing ρ of $\rho \cdot \boldsymbol{\theta}_{diff}^{D=2,4,8,16}$.

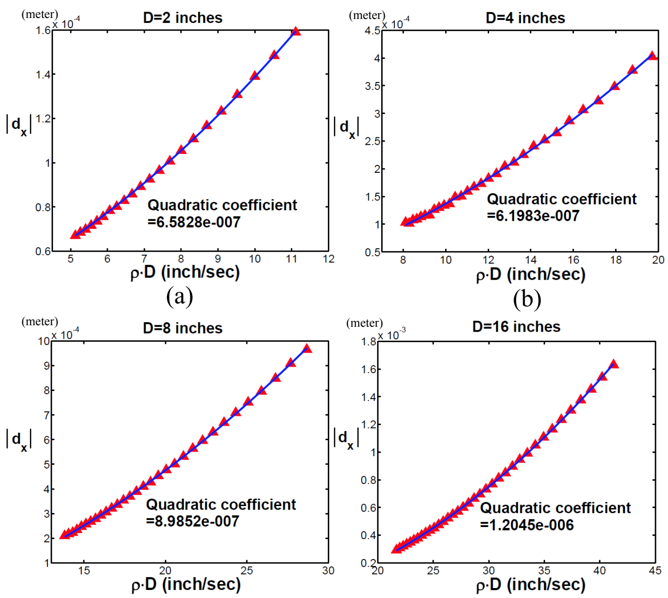

(a) (b) (c) (d)

Fig. 5. Simulation results of the Cartesian position errors of the end-effector of a PUMA 560 robot along the x-axis (d_x) with respect to the Cartesian velocities ($\rho \cdot D$) when $\triangle \boldsymbol{m}$ was -1%. Red triangles represent the simulation results; blue curve represents curve fitting. (a) $D = 2$; (b) $D = 4$; (c) $D = 8$; (d) $D = 16$ inches. All of them had different quadratic coefficients due to the nonlinear relationship between D and joint velocities.

To verify the robot had different motor capabilities with respect to ρ on the x-axis, we changed $\triangle \boldsymbol{m}$, fixed D (i.e $D = 2, 4, 8,$ or 16), and compared the quadratic coefficients among these various $\triangle \boldsymbol{m}'s$. Here, the quadratic coefficients were obtained by curve fitting on the simulation results where x-axis represented ρ. Figure 8 shows the quadratic coefficients when $\triangle \boldsymbol{m}$ was -1%, -0.6%, and -0.2% in each sub-figure where (a), (b), (c), and (d) represent $D = 2, 4, 8,$ and 16. Referring to Figs. 2 and 3, we verified that the quadratic coefficient was $\frac{1}{pI_{px}}$ because a different $\triangle \boldsymbol{m}$ resulted in a different pI_{px}; and among these $\triangle \boldsymbol{m}'s$, we found that the robot with $\triangle \boldsymbol{m} = -0.2\%$ had the largest pI_{px} than $\triangle \boldsymbol{m} = -1\%$ and -0.6%. In other words, the robot with the smaller error between actual and computed masses had the better motor capability. The simulation results validated Eq. (9) because $\left(\boldsymbol{I_x}^T \boldsymbol{J_d}(\boldsymbol{\theta}) \boldsymbol{K} \dot{\boldsymbol{\Phi}}_0^T \triangle \boldsymbol{H}(\boldsymbol{\theta}) \dot{\boldsymbol{\Theta}}_0\right)^{-1}$ and $\triangle \boldsymbol{H}(\boldsymbol{\theta})$ is definitely affected by $\triangle \boldsymbol{m}$.

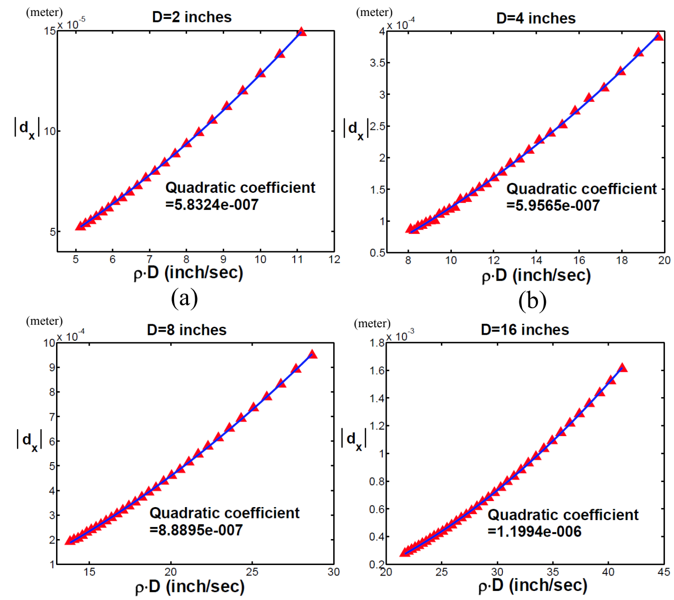

(a) (b) (c) (d)

Fig. 6. Simulation results of the Cartesian position errors of the end-effector of a PUMA 560 robot along the x-axis (d_x) with respect to the Cartesian velocities ($\rho \cdot D$) when $\triangle \boldsymbol{m}$ was -0.6%. (a) $D = 2$; (b) $D = 4$; (c) $D = 8$; (d) $D = 16$ inches.

2) Experiments on a PUMA 560 robot: We experimentally validated the pseudo index of performance on a PUMA 560 robot. For the PUMA 560 robot, we investigated the Cartesian position errors of the end-effector of the PUMA 560 robot caused by the changes of the joint velocities. Figure 9 shows the Cartesian position errors of the end-effector along the x-axis (d_x, the direction of the motion path) with respect to the Cartesian velocities ($\rho \cdot D$). To compare the motor capability of the PUMA 560 robot to a human, points in red show the Cartesian position errors of the end-effector of the PUMA 560 robot at the same $D/T_{mt}{}'s$ as in Fitts' experiment and were approximated by a quadratic trajectory. For example, in Fitts' experiment, when the width of the plate $W_s = 0.25$ inches (allowable Cartesian position error), $D/T_{mt}{}'s$ for $D = 2, 4, 8,$ and 16 were 5.10, 8.26, 13.79, and 21.89 inches/sec, respectively; for $W_s = 0.50$ inches, $D/T_{mt}{}'s$ for $D = 2, 4, 8,$ and 16 were 7.12, 10.75, 17.06, and 26.89 inches/sec, respectively; for $W_s = 1.0$ inch, $D/T_{mt}{}'s$ for $D = 2, 4, 8,$ and 16 were 9.43, 15.38, 22.41, and 33.26 inches/sec, respectively; for $W_s = 2.0$ inches, $D/T_{mt}{}'s$ for $D = 2, 4, 8,$ and 16 were 11.11, 19.70, 28.67, and 41.24 inches/sec, respectively. From

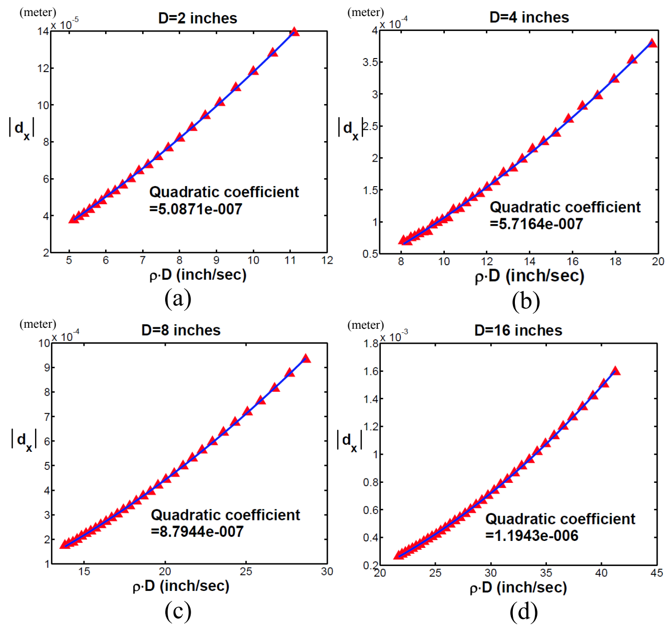

Fig. 7. Simulation results of the Cartesian position errors of the end-effector of a PUMA 560 robot along the x-axis (d_x) with respect to the Cartesian velocities ($\rho \cdot D$) when $\triangle \boldsymbol{m}$ was -0.2%. (a) $D = 2$; (b) $D = 4$; (c) $D = 8$; (d) $D = 16$ inches.

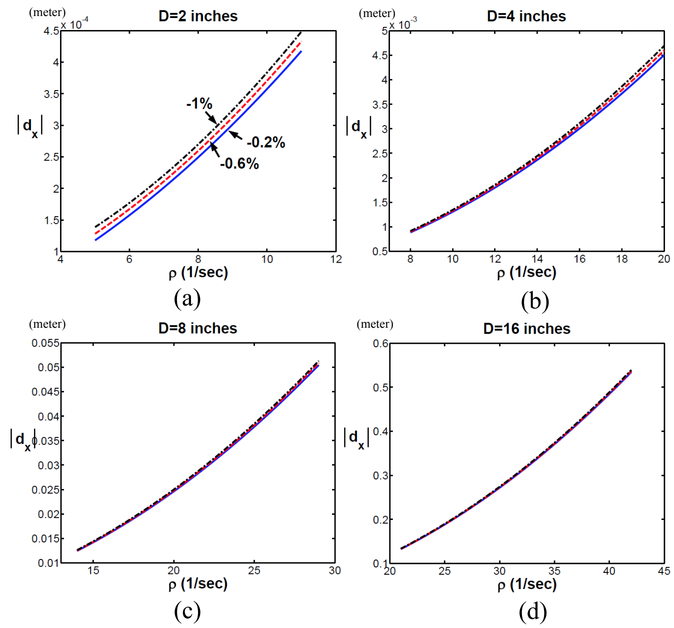

Fig. 8. Simulation results of the Cartesian position errors of the end-effector of a PUMA 560 robot along the x-axis (d_x) with respect to the scalar of the joint velocities (ρ) when $\triangle \boldsymbol{m}$ was -1% (black dot-dash line), -0.6% (red dash line), and -0.2% (blue solid line).

Fig. 9, we found that the Cartesian position errors introduced by the PUMA 560 robot were always smaller than the ones from the human subject in Fitts' experiment at the same D/T_{mt}. In other words, I^r_{px} in Eq. (5) was larger than I_p of the skill performed by the human subject in Fitts' experiment. Thus, it was feasible for the PUMA 560 robot to perform the rapid movement skill from the human subject's demonstration.

V. Conclusions

In this paper, we have presented a quantitative measure, the pseudo index of performance (pI_p), to characterize the motor capability. By using the pI_p, we clearly understand the motor limitation of a robot and facilitate prevalent learning-from-human-demonstration methods to choose an appropriate robot with sufficient motor capability for accomplishing a given task. Computer simulations and experiments with a PUMA 560 robot have validated the characteristics of the pI_p and how the pI_p is utilized to measure the motor capability of a robot for evaluating the feasibility of transferring human rapid aimed movements to the robot.

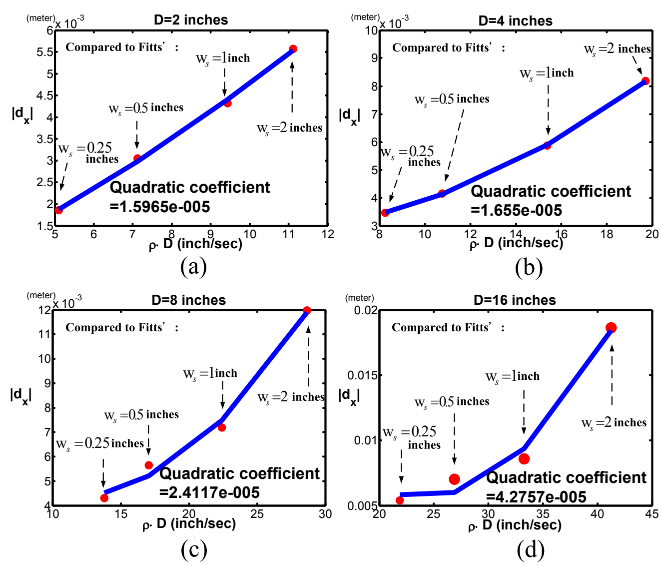

Fig. 9. Experimental results of the comparison of the Cartesian position errors of the end-effector along the x-axis (d_x) with respect to $\rho \cdot D$ between the PUMA 560 robot (red points) and the human subject in Fitts' experiment (${W_s}'s$). (a) D=2 inches; (b) D=4 inches; (c) D=8 inches; (d) D=16 inches.

References

[1] H. I. Lin and C. S. G. Lee, "Skill decomposition by self-categorizing stimulus-response units," in *Proc. IEEE Int. Conf. Robot. Autom.*, May 2008, pp. 3820–3825.

[2] ——, "Self-organizing skill synthesis," in *Proc. IEEE/RSJ Int. Conf. Intell. Robot. Syst.*, Sep 2008, pp. 828–833.

[3] S. Schaal, "Is imitation learning the route to humanoid robots?" *Trends in Cogn. Sci.*, vol. 3, no. 6, pp. 233–242, 1999.

[4] M. Matarić, "Getting humanoids to move and imitate," *IEEE Intell. Syst.*, vol. 15, no. 4, pp. 18–24, July/Aug 2000.

[5] C. Breazeal and B. Scassellati, "Robots that imitate humans," *Trends in Cogn. Sci.*, vol. 6, pp. 481–487, 2002.

[6] P. M. Fitts, "The information capacity of the human motor system in controlling the amplitude of movement," *J. Exp. Psychol.*, vol. 47, pp. 381–391, 1954.

[7] H. I. Lin and C. S. G. Lee, "Speed-accuracy optimization for skill learning," Accepted by Proc. IEEE Int. Conf. Robot. Autom. 2009.

[8] D. E. Meyer, J. E. K. Smith, S. Kornblum, R. A. Abrams, and C. E. Wright, "Speed-accuracy tradeoffs in aimed movements: Toward a theory of rapid voluntary action," *Attention and Performance XIII (edited by M. Jeannerod)*, pp. 173–226, 1990.

[9] P. I. Corke and B. Armstrong-Helouvry, "A search for consensus among model parameters reported for the PUMA 560 robot," in *Proc. IEEE Int. Conf. Robot. Autom.*, May 1994, pp. 1608–1613.

[10] J. Y. S. Luh, M. W. Walker, and R. P. C. Paul, "On-line computational scheme for mechanical manipulators," *J. Dyn. Syst. Meas. & Control (ASME)*, vol. 102, pp. 69–76, 1980.

[11] K. S. Fu, R. C. Gonzalez, and C. S. G. Lee, *Robotics: control, sensing, vision, and intelligence*. New York: Mcgraw-Hill, 1987.